Journal of Thermal Analysis and Calorimetry, Vol. 83 (2006) 2, 439–444

PRELIMINARY STUDY OF THE THERMALLY STIMULATED BLUE LUMINESCENCE OF ULEXITE

V. Correcher[1*], *J. Garcia-Guinea*[2] *and F. J. Valle-Fuentes*[3]

[1]CIEMAT. Av. Complutense 22. Madrid 28040, Spain
[2]Museo Nacional Ciencias Naturales, CSIC. C/ José Gutierrez Abascal 2, Madrid 28006, Spain
[3]Instituto Ceramica y Vidrio, CSIC, Camino Valdelatas, Madrid 28049, Spain

In this paper, novel results on the blue thermally stimulated luminescence (TSL) emission of ulexite ($NaCaB_5O_6(OH)_6{\cdot}5H_2O$) have been studied. The four maxima appearing at 60, 110, 200 and 240°C on the TSL glow curves of this borate could be respectively associated to: (*i*) the first dehydration ($NaCaB_5O_6(OH)_6{\cdot}5H_2O \rightarrow NaCaB_5O_6(OH)_6{\cdot}3H_2O$), (*ii*) the creation-annihilation of the three-hydrated phase, (*iii*) the Na-coordinated chains dehydroxylation and the starting point of the alkali self-diffusion through the lattice and (*iv*) the amorphisation of the lattice. These results are fairly well correlated with the differential thermal analyses (DTA), in situ thermal observations under environmental scanning electron microscope (TESEM) and thermal X-ray diffraction (TXRD) techniques.

Keywords: *amorphisation, dehydration, dehydroxylation, thermoluminescence, ulexite*

Introduction

Boron compounds are widely employed, among others, in the manufacture of glazes, frits and ceramics (B_2O_3), neutron detectors ($^3He/BF_3$ proportional counters) or in the production of synthetic borax. They are often obtained by heating different natural sources of borates such as kernite ($Na_2B_4O_7{\cdot}10H_2O$), colemanite ($Ca_2B_6O_8(OH)_6{\cdot}2H_2O$) or ulexite ($NaCaB_5O_6(OH)_6{\cdot}5H_2O$) producing useful dehydration processes to reduce its mass, decreasing consequently transportation costs. The studies of the thermal decomposition behaviour of borates have commonly been carried out employing X-ray diffraction (XRD), differential thermal analysis (DTA) and thermogravimetry (TG). In fact, during the last 20 years, the thermal dehydration and dehydroxylation of ulexite has been described in several papers [1–5] mainly using DTA and TG data. Sener *et al.* [6] explain as thermal decomposition of ulexite begins at about 60°C and progresses up to 240°C. In the first stage of dehydration, 1.5 mol of H_2O escape at 118°C giving rise to the trihydrate phase ($NaCaB_5O_6{\cdot}3H_2O$, ASTM standard 38–206). The second phase is found in the range 118–260°C appearing two endothermic peaks at 144 and 152°C where 0.5 and 2.5 mol of H_2O are removed during two stages of dehydration. The reaction goes on up to 500°C with dehydration steps and two stages of dehydroxylation. The dehydroxylation step occurs within 180–260°C and at 260°C in which the crystallographic lattice is entirely amorphous. Thus XRD and DTA-TG analyses have extensively been used to describe dehydration-dehydroxylation of ulexite, however, studies on the thermally stimulated luminescence (TSL or TL) emission of ulexite were never achieved before. As known, this method is based on the emission of light from a dielectric solid sample (insulator or semiconductor) when it is heated after being irradiated (naturally or accidentally) by some kind of radiation such as X-rays, gamma rays, beam of electrons, etc. [7]. During the analytical heating, the TL signal is detected by a photomultiplier tube and recorded as a function of temperature or wavelength. The resulting curve is called a TL curve or glow curve; the luminescent intensity and the shape of this glow curve are functions of radiation dose and heating rate. Thermoluminescence provides helpful information on*:* (*i*) trapped charge recombination sites related to metastable defects inside the lattice [7], (*ii*) phase transitions [8], (*iii*) consecutive breaking and linking of bonds including redox reactions, dehydroxylation and dehydration processes [9] and (*iv*) thermoinduced alkali self-diffusion produces mass transport which may be the dominant mechanism for sub-critical crack growth [10]. TL is usually employed in the field of radiation dosimetry and dating of ancient archaeological pottery samples as well as of geological samples. All the factors involved in the luminescence phenomena (i.e. lifetime, efficiency, emission spectra, etc.) depend directly on the crystalline phase which is mainly influenced by pressure and tempera-

* Author for correspondence: v.correcher@ciemat.es

1388–6150/$20.00

Akadémiai Kiadó, Budapest, Hungary
Springer, Dordrecht, The Netherlands

ture. In this paper novel and preliminary results concerning the TL emission of ulexite are reported. The maxima appearing in the TL glow curve, associated to thermal transformations during heating, are compared to DTA, thermal environmental scanning electron microscope (T-ESEM) and thermal X-ray diffraction (TXRD) results.

Experimental

Ulexite samples from the Boron Mine (U.S. Borax Corporation, Boron, California), were selected from the collection of the Museo Nacional Ciencias Naturales (Madrid, Spain).

Samples were analysed under environmental scanning electron microscope (ESEM) in a Philips XL30 model ESEM employing a GSED detector to visualize the modifications on the surface of the hydrated lattice structure. A layer of 0.2 mm of ulexite sample was placed directly onto a clean refractory ceramic surface, which was fixed to the ESEM stainless steel support. The measurements were carried out in environmental conditions to study the dehydration-dehydroxylation processes. The pressure in the chamber was reduced to 2 Torr, involving a 10% of relative humidity. Later, the temperature of the stage was increased from room temperature (rt) at 19 to 500°C. The TXRD measurements were performed in a home-made door used for the experiments that permit modern electronic supplies to be plugged into the X-ray chamber [11]. Electric resistances, thermocouples, and halogen lamps were coupled with the wide old X-ray cameras while maintaining the usual management of the X-ray diffractometer. This device uses a set of self-improvements to mechanical supplies, electronic circuits and software to upgrade a classic X-ray diffractometer Philips PW1710/00, as follows: (a) a new original water refrigerator, (b) a new stainless steel door able to hold internal cooling fluids, (c) internal heaters in new sample-holders, under proportional-integral-derivative (PID) control and a RS232-PC-computer which also controls the cooling fluid electro-switch, (d) a new electronic circuit and software to record DTA analyses between sample and reference, at 50 temperature data measurements per second in continuum. The automatic temperature control loop consists of a thermocouple for measuring the temperature, a precision temperature controller with auto-tuning (Eurotherm model 2216) and a thyristor power regulator operating in phase angle. To manage the Eurotherm thermal controller, the thyristor unit, the relay of the cooling fluid flows by a serial RS232 port and a marketable ITOOLS v.2.09 (Windows-98) program from Eurotherm, U.K. were installed. The resulting electrical signal, which is the difference between the welding of both thermocouples, is plugged into an analogical-digital 22 bits circuit (Analog Devices AD7710 ADC) regulated by a micro-controller PIC16F84 of Microchip Technology Inc. (μC). DTA measurements were carried out in a STA 409, Netzsch-Geratebau model (Selb-Bayern, Germany) using a sample weight of about 80 mg in open air, and heating rate of 1°C min^{-1}.

The TL measurements were performed using an automated Risř TL system model TL DA-12 [12], this reader is provided with an EMI 9635 QA photo-multiplier and the emission was observed through a blue filter (FIB002 Melles-Griot) with transmission in the 320–480 nm range; FWHM is 80±16 nm and peak transmittance is 60%. It is also provided with a $^{90}Sr/^{90}Y$ source with a dose rate of 0.020 Gy s^{-1} calibrated against a ^{60}Co photon source in a secondary standards laboratory [13]. The TL measurements were performed at 5°C s^{-1} from room temperature to 450°C in a N_2 atmosphere. Four aliquots of 5.0±0.1 mg each of ulexite were used for each measurement. The sample was carefully powdered with an agate pestle and mortar to avoid triboluminescence [14]. The incandescent background was subtracted from the TL data.

Results

The natural blue TL emission (i.e. emission of the 'as received' sample without thermal or irradiation pre-treatments) of powdered ulexite is characterized by a low photon intensity never higher than 50 arbitrary units (per 5 mg of powdered sample) indicating that this material is no sensitive enough to the natural radiation exposure (Fig. 1). According to the curve, it is possible to distinguish four different maxima peaked at 60, 110, 200 and 240°C. The explanation of the process that takes place in ulexite to produce the

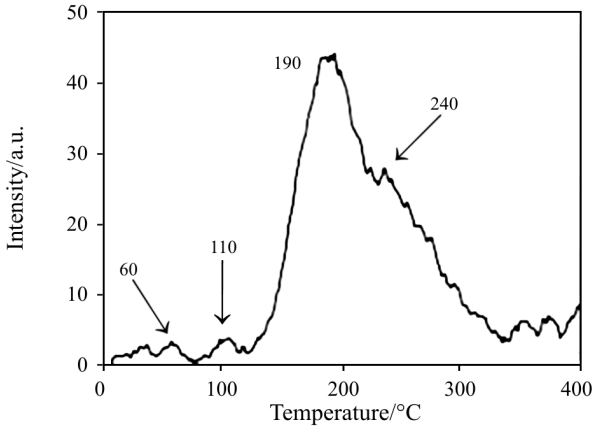

Fig. 1 Blue thermoluminescence glow curve of a natural powdered ulexite from Boron (California) loaded at 5°C s^{-1}

first TL peak (at 60°C) is supported by the obtained TXRD results (Figs 2 and 3). In this sense, the XRD profile at room temperature (i.e., 20°C, in open-air conditions) displays well-defined peaks coming from the (010), (100), (1̄10) and (110) planes (Fig. 2a). When the temperature of the sample is increased at 40–50°C no significant changes could be observed; however, it is possible to detect the fading of two small peaks circa 5.6 (2θ) and 10.7 (2θ) when ulexite is heated at 51°C for 13 h (Fig. 2b). At higher temperatures, in the range of 50–59°C, two different effects can be distinguished firstly, a split of the (010) and (1̄10) peaks and secondly, the intensity of the (010), (100) (1̄10) and (110) planes that starts to decrease after four hours at 59°C. These structural changes at low temperature (below 60°C) could be explained by water loss from the ulexite lattice. Figure 3 displays a set of isothermal sequential XRD profiles with a progressive increasing of temperature. Sets of isothermal XRD profiles at 60°C in the X-ray chamber, in dry conditions, confirm fast changes in the first hour with a large reduction of the intensity of the XRD (010) peak showing a low stability of the ulexite structure at this temperature. Four hours later, it is possible to appreciate three specific changes: (*i*) a progressive angular displacement of the (1̄10) XRD maximum, (*ii*) melting away the 11–12° (2θ) peaks and (*iii*) growth of the (100) peak. Assuming that both Ca-coordinated

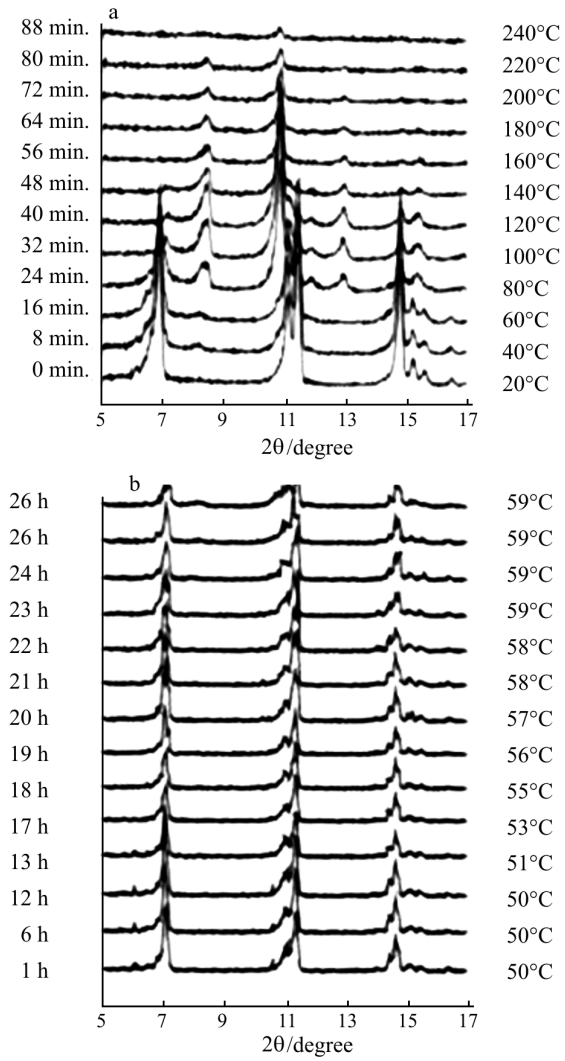

Fig. 2 a – Sequential non-isothermal X-ray profiles of ulexite showing: ulexite (circa 20–60°C), three-hydrated phase (circa 80–160°C) and amorphous-end (240°C) b – Detailed sequential non-isothermal X-ray profiles of ulexite showing: removal of the 6°(2θ) peak at 51°C and the starting point of the pulling down of the ulexite lattice (59°C)

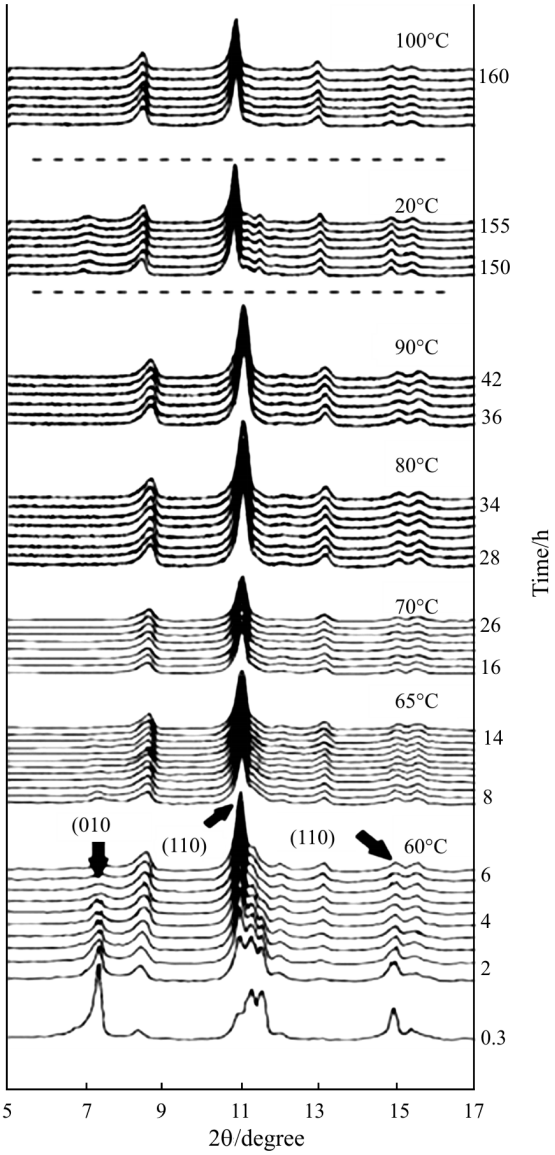

Fig. 3 Sequential non-isothermal sets of X-ray profiles of ulexite: major structural changes are produced at 60°C, at higher temperature than 60°C the new three-hydrated phase is reasonably stable. Note the neo-formation of new ulexite by deliquescence at 20°C after 5 days

and Na-coordinated chains run parallel to *c*, the fibre-axis optical direction, these thermal changes in the ulexite structure could be associated to breaks along {010} and leakage of structural water. In the same process, many diffracting powder particles seem to be re-orientated from {010} to {100}. This initial dehydration of separated ulexite fibres could explain the observation made in the US Geological survey [15] in which some single crystals of ulexite remain clear as long as they are stored with others but, when isolated, appear to be altered. With a mild heating from room temperature to 60°C, natural ulexite partially dehydrates to a new crystallographic structure giving rise to the three-hydrated phase ($NaCaB_5O_6(OH)_6{\cdot}3H_2O$; ASTM card file 38–206). Looking for the thermal stability of this three-hydrated phase, the aliquot was heated in progressive isothermal recordings at 60, 65, 70, 75, 80 and 90°C for 40 h. After 160 isothermal TXRD profiles obtained during five days, the structure of the ulexite displays a very high stability. However, in the next experiment, started with the same aliquot (Fig. 3, 20°C), a small amount of neo-formed ulexite phase was identified in the XRD profiles. It means that after dehydration process produced at 60°C (i.e. a maximum of temperature reached similar to the more extreme sunlight exposure), one can assume that natural ulexite is newly re-hydrated by deliquescent mechanisms. For these reasons, the TL peak appearing at 60°C could, therefore, be associated to the partially first dehydration ($NaCaB_5O_6(OH)_6{\cdot}5H_2O \rightarrow NaCaB_5O_6(OH)_6{\cdot}3H_2O$) that is the starting point of the longitudinal breaking of the optical fibres (see Fig. 4). Thus, the in situ study performed under ESEM reveals the appearance of some modifications on the surface of the mineral from rt to 500°C, that grows unidirectional in tiny transparent parallel bundles of filaments that transmit light, rather like fibre optics. During the thermal treatment, the large spaces among the sodium octahedrally chains into the ulexite lattice observed at rt (Fig. 4a) are modified. The light transmission of the ulexite crystals can be explained in terms of fibre-optics [16], designating as core the crystals aligned along the c direction of the fibre with index g approximately 1.529 and they show that cladding results from random orientations of crystals about the fibre direction, producing a core-to-cladding index difference ranging from 0 to a maximum of $\gamma-\alpha=0.038$. According to Ghose *et al.* (1978) [15], the ulexite domain corresponds to triclinic Pl structure. At room temperature, the basic boron polyanion unit $[B_5O_6(OH)_6]^{3-}$ is composed of three borate tetrahedrons and two borate triangular groups. The structure contains three different groups: isolated pentaborate polyanions, Ca-coordination polyhedral and Na-coordination octahedral chains, all cross-linked by hydrogen bonds. The Ca-coordination polyhedral share edges to form chains which are separated from the Na-coordination octahedrally chains; the pentaborate polyanions sandwich between the two kinds of chains to help link them together; all chains run parallel t) *c*, the fibre-axis optical direction. These chains dominate the structure being responsible for the fibrous habit of ulexite. The increase of temperature from 60 to 120°C leads to a complete phase transition between the pentahydrated ulexite and a three-hydrated phase and the appearance of the second TL maximum, peaked at 110°C that could be linked to the formation-annihilation of this three-hydrated phase. The study carried out under T-ESEM demonstrates how the fibres forming the ulexite structure starts to be disjoined along the longitudinal direction when the temperature raises (Fig. 4b).

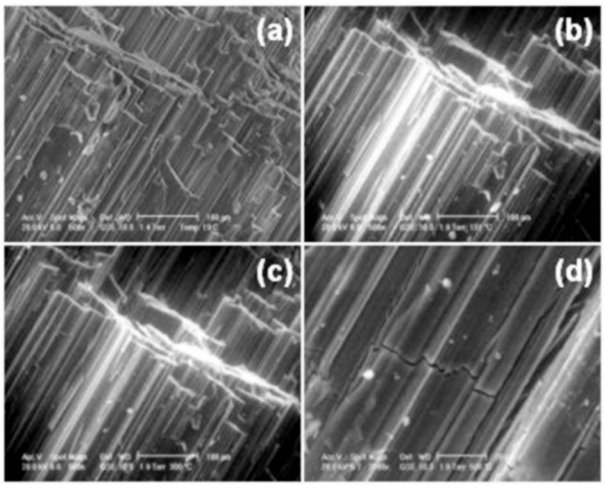

Fig. 4 Environmental scanning electron microscope (ESEM) image of the ulexite fibers running parallel to c, the fiber-axis optical direction Ca-polyhedral and Na-octahedral chains dominate the structure and are responsible for the fibrous habit of ulexite at a – 19, b – 131, c – 300 and d – 500°C

The gradual enhancement of temperature (from 120°C onwards) induces progressively dehydration, dehydroxylation and alkali self-diffusion processes through the lattice as detected by means of TXRD, DTA and T-ESEM. Thus, from circa 120°C, the lower TXRD intensity of several peaks indicates that the three-hydrated phase tends to amorphisation at approximately 260°C in which the profile is virtually flat (Fig. 3a).

As illustrated in Fig. 5, this borate exhibits two DTA endothermic peaks at 130 and 180°C associated respectively to a dehydration and dehydroxylation processes. These two DTA endothermic peaks could be partially interpreted as two different types of water losses; the first one stems from the natural ulexite structure and the second one, at 180°C, from the

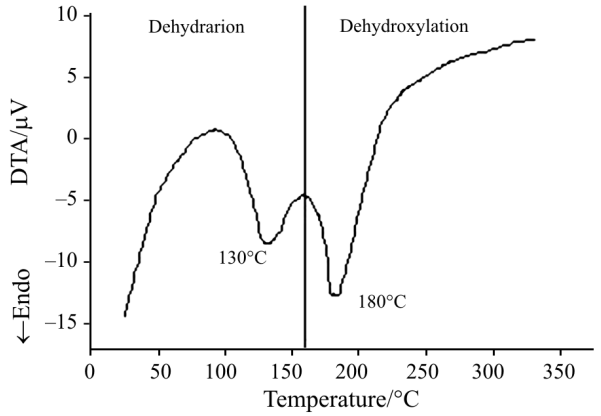

Fig. 5 Differential thermal analysis of natural powdered ulexite obtained at a heating rate of 1°C min^{-1} from room temperature to 350°C showing endothermic peaks at 130 and 180°C that can be respectively attributed to a dehydration and dehydroxylation processes

three-hydrous lattice in coincidence with its maximum volume of water leaking. No other additional hydrous phases of $NaCaB_5O_6(OH)_6$ were identified by TXRD. From the view of the bond strength of bonds in the framework, the OH^- groups are more strongly bonded with Ca^{2+} (bond energy 442 kJ mol^{-1}) than Na^+ (358 kJ mol^{-1}) cation; moreover all types of OH^- and the last H_2O losses must be included in the complex second DTA endothermic peak. In general, due to their higher oxidation states (double number of bonds and/or ionic charge), the dissociation energies of alkaline earth metal compounds in the solid state are higher than dissociation energies for the alkali metals compounds. It could be observed that the ulexite dehydration-amorphisation process of the Na-coordinated OH^- starts from 130°C and must be completed below 500°C, temperature in which the new lattice of $NaCaB_5O_9$ (ASTM 37-827) grows from the amorphous-anhydrous material.

Over 300°C (Fig. 4c), under ESEM is possible to detect several transformations in the structure caused by the thermal treatment. The fibres are disjoined when increased the temperature along the longitudinal direction and this is followed by the production, at higher temperatures (500°C, Fig. 4d), of secondary transverse cracks which combined to the longitudinal cracks give rise a grid pattern. These fractures should correspond to the amorphisation of the structure detected by TXRD. This means that the third TL peak could be mainly related to (*i*) total annihilation of the three-hydrated phase and (*ii*) the alkali self-diffusion through the lattice due to consecutive breaking linking of Na–OH and Ca–OH bonds; and the fourth TL emission could be interpreted as different pulses of the dehydroxylation, mainly Na-coordinated, from residual crystallographic relicts of ulexite chains into a generalised amorphous mass.

Discussion

The model here proposed to explain the TL curve of natural ulexite, that is fairly well correlated with XRD and DTA results, could be also ratified by mechanoluminescence (ML) or triboluminescence mechanisms in which the physical transformations of crystals give rise to photon emission. Assuming that at low temperature the processes of dehydration, phase-transition and light emission occurs in natural fibrous ulexite, in the same aliquot-temperature-time, from room temperature to 260°C, the TL definition of ulexite does not seem to be fitted in a simple electron-hole model. In fact, thermally induced blue TL emissions of ulexite cannot be explained employing the commonly accepted model based on the discrete trap distribution model since it was not possible to determine some physical parameters such as trap-energies or pre-exponential factors. These TL curves were analysed in terms of either first (where the intensity of the TL is proportional to the concentration of thermally released charges) and second (the thermally released charges are retrapped at least once before the recombination process) order kinetics equations. However the best fit parameters obtained, based on the value of the factor of merit, were unsatisfactory. Therefore, due to the complexity of the natural TL glow curves, speculation on a structure of a continuous trap distribution, as in other mineral phases involving multiorder kinetics, might be considered.

Furthermore, it seems to be obvious that relationships between dehydration and the structural collapse the bundles of ulexite fibres exist. Following a ML classification [17], ulexite exhibits thermally induced dislocation electrostatic interaction and thermal excitation tribo-ML processes that should be kinetically presented by four different steps: (1) splitting of the structural ulexite chains and loss of two water molecules since 60°C; (2) creation-annihilation of the three-hydrated phase of the neo-formed crystallographic structure ($NaCaB_5O_6(OH)_6{\cdot}3H_2O$; ASTM card file 38–206) finishing circa 130°C; (3) additional dehydration-dehydroxylation from the Na-coordinated chains up to a whole amorphisation circa 260°C. This thermal evolution, involving phase-transitions, includes synchronous processes of ML emission, crack nucleation and propagation and could be linked to the fractures in the structural chains of ulexite. The dislocation motions produced during the plastic deformation of crystalline materials induces light emission due to several processes: (*i*) mechanical or electrostatic interaction of dislocations with defect centres, (*ii*) the breakdown of adsorbed water molecules and (*iii*) the generation of holes during the decay of mobile dislocations on the surface of crystals. The physical process here observed for ulexite is

quite similar to other model described for the desiccation of mudstone water-kaolinite that also produces dehydration-induced luminescence [18].

Natural powdered ulexite displays a complex blue TL glow curve, with a little maximum at 60°C from the first dehydration; a second peak circa 110°C, linked to the annihilation of the three-hydrated and a large TL emission arising from 130 to 200°C associated with dehydroxylation of Na-coordinated chains. During the thermal gap of TL measurements, i.e., from room temperature to 400°C, the ulexite lattice suffers water loss and dehydroxylation processes that must be associated with light emissions. As observed in kaolinite [19], photon emission may be associated with the formation of micro-cracks and their propagation during the dehydration period. The sub-critical crack growth can be due to several competing mechanisms, such as stress corrosion, diffusion, dissolution, or micro-plasticity. Diffusion properties of minerals are often controlled by the effect of minor amounts of water. The response of minerals to ionising radiation is also influenced by hydrous components. To complete this preliminary results, the research for future should be focused on two specific aspects: (*i*) study of the correlation between TL emission and EPR measurements of this borate to obtain information about electron-hole centers involved in TL processes and (*ii*) study of each peak based on the wavelength spectral emission.

Conclusions

The increase in the temperature is the case of several modifications in the ulexite structure as noted by means of TL, TXRD, DTA and TESEM. The TL results of fibrous ulexite here presented are basically agree with previous data following ML kinetics of thermal decomposition of hydro-borates which depends on the geometry of the crystal lattice, chemical bonds, grain size, crystal morphology, lattice defects and pressure of gaseous products. The appearance of the four TL maxima is mainly produced by successive structural transformations observed onto the surface of the sample during the thermal treatment. The TL glow peaks appearing at 60, 110, 200 and 240°C could be respectively linked to: (*i*) the first dehydration ($NaCaB_5O_6(OH)_6{\cdot}5H_2O \rightarrow NaCaB_5O_6(OH)_6{\cdot}3H_2O$) detected under TXRD due to a split of the (010) and ($\bar{1}10$) peaks of the structural ulexite chains, (*ii*) the creation-annihilation of the three-hydrated phase of the neo-formed crystallographic structure ($NaCaB_5O_6(OH)_6{\cdot}3H_2O$; ASTM card file 38-206), (*iii*) the Na-coordinated chains dehydroxylation and the starting point of the alkali self-diffusion through the lattice and (*iv*) the amorphisation of the lattice.

Acknowledgements

This work has been supported by the BFM2002-00048 and CGL2004-03564/BTE CICYT projects.

References

1 L. Stoch and I. Waclawska, J. Thermal Anal., 36 (1990) 2045.
2 H. Ersahan, M. Tunc, A. Ekmekyapar and S. Yapici, Thermochim. Acta, 250 (1995) 125.
3 R. Chen, J. Li, S. Xia and S. Gao, Thermochim. Acta, 306 (1997) 1.
4 M. Tunc, H. Ersahan, S. Yapici and S. Colak, J. Thermal Anal., 48 (1997) 403.
5 Y. Erdogan, A. Zeybek, A. Sahin and A. Demirbas, Thermochim. Acta, 326 (1999) 99.
6 S. Sener, G. Ozbayoglu and S. Demirci, Thermochim. Acta, 362 (2000) 107.
7 S. W. S. McKeever. Thermoluminescence of solid, Cambridge Univ. Press, Cambridge, 1985, p. 32.
8 V. Correcher, J. Garcia-Guinea, P. Lopez-Arce and J. M. Gomez-Ros, Spectrochim. Acta A., 60 (2004) 1431
9 V. Correcher, J. M. Gomez-Ros, J. Garcia-Guinea and A. Delgado, Nucl. Instrum. Methods A., 528 (2004) 717
10 J. Garcia-Guinea, V. Correcher, M. Lombardero and R. Gonzalez-Martin, Int. J. Environ. Heal. R., 14 (2004) 285.
11 J. Garcia-Guinea, R. Ortiz, V. Correcher, A. LaIglesia and J. D. Martín-Ramos, Rev. Sci. Instrum., 72 (2001) 4005.
12 L. Bŕtter-Jensen and G. A. T. Duller, Nucl. Track. Radiat. Meas., 20 (1992) 549.
13 V. Correcher and A. Delgado, Radiat. Meas., 29 (1998) 411.
14 J. Garcia-Guinea and V. Correcher, Spectrosc. Lett., 33 (2000) 103.
15 S. Ghose, C. Wan and J. R. Clark, Am. Miner., 63 (1978) 160.
16 E. J. Weichel-Moore and R. J. Potter, Nature, 200 (1963) 1163.
17 B. P. Chandra, Radiat. Eff. Defect. Solids, 138 (1996) 119.
18 N. Lahav, L. Coyne and J. G. Lawless, Clays Clay Miner., 3 (1985) 207.
19 J. Garcia-Guinea, V. Correcher and F. J. Valle-Fuentes, Radiat. Protect. Dosim., 84 (1999) 507.

Received: May 5, 2005
Accepted: November 10, 2005

DOI: 10.1007/s10973-005-7122-9